International Journal of Mass Spectrometry 299 (2011) 9–12

Contents lists available at ScienceDirect

International Journal of Mass Spectrometry

journal homepage: www.elsevier.com/locate/ijms

Fluoride affinities of fluorinated alanes

Jamelle K.P. Williams, Paul G. Wenthold *

The Department of Chemistry, Purdue University, West Lafayette, IN 47907, United States

ARTICLE INFO

Article history:
Received 4 June 2010
Received in revised form 3 September 2010
Accepted 3 September 2010
Available online 15 September 2010

Keywords:
Energy-resolved mass spectrometry
Flowing afterglow
Alane
Thermochemistry
Fluoride affinity

ABSTRACT

The fluoride affinities of fluorinated alanes, AlH_mF_{3-m} (m = 1–3) were measured using energy-resolved collision-induced dissociation of fluorinated aluminate anions. The $AlH_mF_{4-m}^-$ anions were formed by reaction of dimethylethylamine-alane with fluoride ion and F_2. From the measured bond dissociation energies, the fluoride affinities of fluorinated alanes are determined to be 93.2 ± 3.1, 97.5 ± 4.0, and 108.6 ± 3.7 kcal/mol for m = 3, 2, and 1, respectively. The fluoride affinities are in good agreement with the theoretical calculations at the CCSD(T)/CBS and B3LYP/6-31 + G* levels of theory. The increased Lewis acidity of more fluorinated alanes is attributed to increased positive charge density on the aluminum.

1. Introduction

Thermochemical properties provide fundamental insight into the nature of molecular structure and bonding [1]. There are a wide variety of commonly measured thermochemical properties such as proton affinities, gas-phase acidities, and electron and hydride affinities. Fluoride affinity (FA) is also an important thermochemical property, serving as a measure of the Lewis acidity. The measurements of FAs have been determined experimentally using a variety of techniques [2–4]. Haartz and McDaniel used ion cyclotron resonance spectroscopy to determine the relative order of the fluoride affinity to be SF_4, $SF_5 < SO_2$, HCl, $AsF_3 < SiF_4 < BF_3 < PF_5 < BCl_3 < ASF_5$ [2]. Larson and McMahon related fluoride affinities to the hydrogen bond strengths of various chemical species [3], which enabled them to create a wide-range fluoride affinity scale. The scale was fixed at the low end with the fluoride affinity of H_2O (23.3 kcal/mol) and at the high end with the fluoride affinity of HCO_2H (45.3 kcal/mol). Energy-resolved collision-induced dissociation (CID) has led to revisions of the fluoride affinity scale allowing the addition of new values [4–6].

Despite the advancement in FA measurements, very few aluminum containing systems have been studied. In fact, few thermochemical properties are known for any aluminum containing molecules, alanes in particular. Aluminates such as aluminum hydride are important because they are commonly used as reducing agents and have been proposed as a means for hydrogen storage [7]. In this study, we determined the fluoride affinities of fluorinated alanes using a flowing afterglow-triple quadrupole instrument.

2. Experimental

2.1. Instrumental description and data analysis

The fluoride affinities of fluorinated alanes were determined using a flowing afterglow-triple quadrupole mass spectrometer that has been previously described elsewhere [8]. Fluoride ions were generated by 70 eV electron ionization of F_2 (5% in helium). Helium buffer gas (P = 400 mTorr) was used to carry the ions through the flow tube at a flow rate of ca. 190 STP cm^{-3}/s. Ions were then allowed to undergo ion-molecule reactions with the neutral reagent (dimethylethylamine-alane, DMEAA) added through a reagent port, down stream the flow tube. Ions were then extracted through a 1 mm nose cone orifice into the triple quadrupole mass analyzer where they were analyzed.

Collision-induced dissociation (CID) was carried out by mass selecting the ion of interest in the first quadrupole. The ions enter the second quadrupole and subsequently collide with xenon target gas. The higher mass and polarizability of xenon as the target gas leads to a more efficient kinetic-to-internal transfer in the CID process [9]. The resulting fragment ions were extracted into the third quadruple where they were detected with a conversion dynode and an electron multiplier, which is operated in the pulse counting mode. During energy-resolved mass spectrometry experiments, product formation is measured while the q2 offset is scanned over a range of energies. The products are analyzed in q3.

* Corresponding author at: Department of Chemistry, Purdue University, 560 Oval Drive, West Lafayette, IN 47907, United States.
Tel.: +1 765 494 0475; fax: +1 765 494 0239.
E-mail address: pgw@purdue.edu (P.G. Wenthold).

1387-3806/$ – see front matter © 2010 Elsevier B.V. All rights reserved.
doi:10.1016/j.ijms.2010.09.003

The cross sections (σ) were calculated using $\sigma_p = I_p/INl$, where N is the number density of the target and l is the effective length of the collision cell, calibrated to be 24 ± 4 cm [8]. The effective path length was obtained from calibration experiments using the reaction of $Ar^+ + D_2$, which has a well established cross section [10]. I_p and I are the intensities of the parent ions and the product ions, respectively. The center of mass collision energies were calculated using $E_{cm} = E_{lab}/[m/(M+m)]$, where E_{lab} is the collision energy under laboratory frame, m is the mass of the target and M is the mass of the ion. The cross sections were measured at different pressures and extrapolated to zero pressure, which corresponds to single ion collision conditions.

Energy-resolved cross sections are fitted using model shown in Eq. (1) [11,12]. In this equation, σ_0 is a scaling factor, g_i is the fraction of ions with the internal energy E_i, E is the center of mass energy of the reactant ion, E_0 is the threshold energy for dissociation, and n is an adjustable parameter that reflects the energy deposition in the collision. The parameter P_i is the probability calculated using RRKM theory. The data are modeled by changing the parameters to fit the linear part of the appearance curve. The rotational constants and vibrational frequencies, needed to determine the internal energy of the ion, were calculated using Gaussian 03 at B3LYP/6-31 + G* level of theory [13]. Data analysis and modeling were carried out using the CRUNCH program [14–16].

$$\sigma(E) = \sigma_0 \sum \frac{P_i g_i (E + E_i - E_0)^n}{E} \quad (1)$$

2.2. Computational methods

Geometries and energies of the fluorinated alanes and fluorinated aluminate ions were calculated at the B3LYP/6-31 + G* [13] and CCSD(T) [17] levels of theory. Theoretical fluoride affinities were calculated using an isodesmic approach, calculating the 298K enthalpy for the fluoride transfer reaction with tetrafluoroaluminate, shown in Eq. (2).

$$AlF_4^- + AlH_{3-m}F_m \rightarrow AlF_3 + AlH_{4-m}F_m^- \quad (2)$$

Absolute fluoride affinities for the aluminum hydride ion are obtained by combining the computed enthalpy of reaction (2) with the fluoride affinity of AlF_3, 116.7 ± 2.4 kcal/mol [18]. Coupled-cluster energies of the alanes and aluminates were calculated using the aug-cc-pVDZ, aug-cc-pVTZ and aug-cc-pVQZ basis sets, using the CCSD(T)/aug-cc-VDZ geometries. The CCSD(T) energies were extrapolated to the complete basis set (CBS) limit using the standard relationship shown in Eq. (3) [19].

$$E(x) = E_\infty + AX^{-3} + BX^{-5} \quad (3)$$

Zero point energy and thermal corrections to the CCSD(T) energies were obtained using the unscaled B3LYP/6-31 + G* frequencies. The total corrections are less than 0.1 kcal/mol for the reaction in Eq. (2).

2.3. Materials

Unless otherwise indicated, reagents were used as received without further purification. Fluorine gas (5% in helium) was purchased from Spectra Gases. A 0.5 M solution of dimethylethylamine-alane (DMEAA) in toluene was obtained from Sigma–Aldrich.

3. Results

Fluorinated aluminate ions were generated by chemical ionization (CI) of the Lewis acid–base complex dimethylethylamine-alane, DMEAA, with F^- generated from F_2 as the CI reagent Eq. (4). Among the products observed are $AlH_mF_{4-m}^-$, where $m = 0$–3. By changing the source conditions, more of the higher masses can be formed ($m = 1, 2$). The fourth ion, AlF_4^- could not be formed in sufficient abundance for CID studies. AlH_3F^- is likely generated by substitution of the dimethylethylamine in DMEAA. The more highly substituted fluorinated ions are likely formed by the reaction of AlH_3F^- with fluorine gas. Upon CID, the ions lose fluoride ion as the only product, leaving a neutral substituted alane Eq. (5). Fluoride affinities of fluorinated alanes were measured directly using energy-resolved CID.

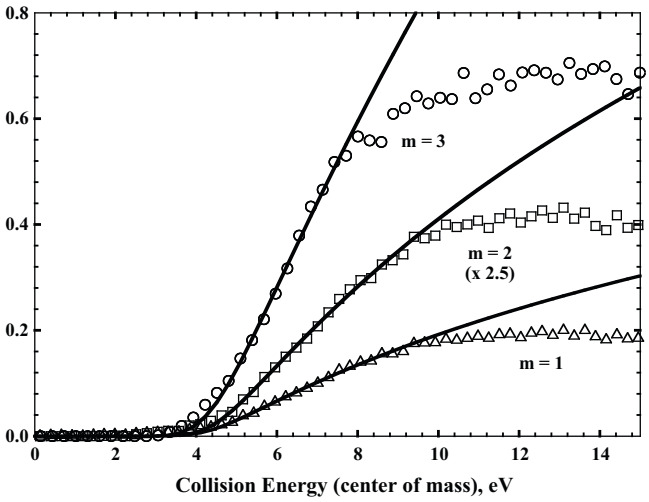

Fig. 1. Absolute cross sections for CID of $AlH_mF_{4-m}^-$ ions as a function of collision energy. The circles ($m = 3$), squares ($m = 2$), and triangles ($m = 1$) represent the formation of fluoride. The solid lines are the fully convoluted fits for the data.

$$C_2H_5N(CH_3)_2{\cdot}AlH_3 + F^-/F_2 \rightarrow AlH_mF_{4-m}^- \quad (4)$$

$$AlH_mF_{4-m}^- \rightarrow AlH_mF_{3-m} + F^- \quad (5)$$

The cross sections for the formation of fluoride as a function of energy are shown in Fig. 1. Even at the highest energy, the measured cross sections are very small. While the reactions are undoubtedly inefficient because of the high bond dissociation energies, it is also the case that low-mass ions are discriminated against in the flowing afterglow-triple quadrupole [20]. The solid lines are the convoluted fit to the data, obtained using the procedures explained in the experimental. From the modeling, the bond dissociation energies for the formation of F^- are found to be 93.2 ± 3.1, 97.5 ± 4.0, and 108.6 ± 3.7 kcal/mol for $m = 3$, 2, and 1, respectively, where uncertainties include the uncertainty in the absolute energy scale for the experiment (± 0.15 eV lab frame), the standard deviation of values obtained from replicate experimental trials, and uncertainty from error in the transition state. Error in the transition state is estimated as the change in the dissociation energy that results when the frequencies are scaled to change the activation entropy by ± 2 cal/mol K, and is ca. 0.01 eV. The measured fluoride affinities of the alanes are listed in Table 1. Not surpris-

Table 1
Experimental and calculated fluoride affinities (kcal/mol).

	Experimental	Calculated	
		CCSD(T)/CBS	B3LYP/6-31 + G*
AlH_3	93.2 ± 3.1	93.3	89.0
AlH_2F	97.5 ± 4.0	99.4	95.9
$AlHF_2$	108.6 ± 3.7	106.8	104.9
AlF_3	116.7 ± 2.4[a]	116.7[b]	116.7[b]

[a] Ref. [19].
[b] Obtained using the isodesmic approach Eq. (2), anchored to the FA of AlF_3, 116.7 kcal/mol.

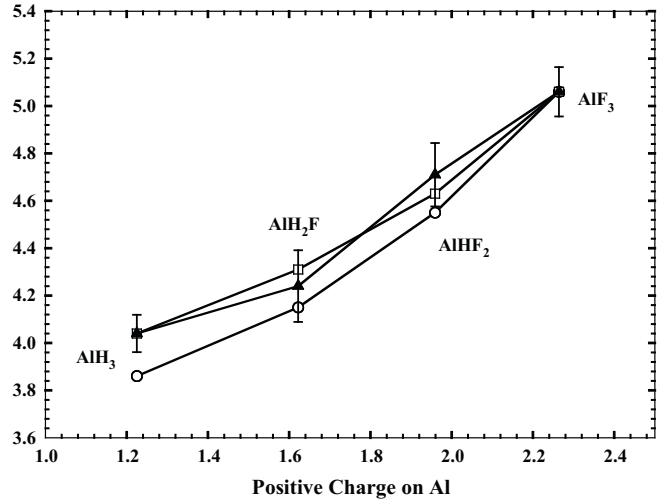

Fig. 2. Plot of experimental and calculated fluoride affinities of the alanes versus the calculated (NPA) charge on the aluminum. The solid triangles are the experimentally measured values, with error bars, whereas the squares and circles are values computed at the CCSD/CBS and B3LYP/6-31 + G* levels of theory, respectively.

ingly, the fluoride affinities are larger for alanes with more fluorine substitution.

The computed FAs, obtained using the isodesmic procedure and anchored to that for AlF_3, are provided in Table 1. Calculated bond lengths and bond angles in the fluorinated alanes and aluminates are provided as Supplementary data.

4. Discussion

The experimentally measured FAs are in good agreement with the theoretical predicted values, with only the B3LYP value for $AlHF_2$ at the edge of the assigned error limit. As noted above, the FA values are larger for alanes with more fluorine substituents, reflecting the greater Lewis acidity for these substrates. The increased Lewis acidity results from increased positive charge density on the aluminum in the alane when replacing a hydrogen atom with a more electronegative fluorine. Charge densities in the alanes were calculated using natural population analysis (NPA) of the CCSD/aug-cc-pVTZ wave function [21–23]. The positive charge on the aluminum was found to be 1.22, 1.63, 1.93, and 2.21 for AlH_3, $AlHF_2$, and AlH_2F, and AlF_3, respectively.

A plot of the FA versus positive charge density on aluminum, Fig. 2, shows a strong correlation between FA and charge density. If fluoride binding were simply a Coulombic interaction, then there should be a linear relationship between FA and charge density. With the uncertainties on the experimental values, a linear relationship cannot be ruled out. The computed values suggest that it is not completely linear, with disproportionately higher FA values with larger charges. However, some of the deviation can be attributed to geometry differences. The Al–F bond distances in the aluminates (Supplementary data) are shorter when more fluorines are present, which would lead to a stronger Coulombic interaction. However, the difference in geometries is not sufficient to account for all of the non-linearity of the computed values.

Additional insight can be obtained by considering the absolute electronic energies of the fluorinated alanes and aluminum hydride anions (Supplementary data). In particular, the energies can be used to assess in light of the extent of fluorination of the alanes and aluminate anions. For example, the effect of fluorination on the aluminate anions is nearly additive after the addition of the first fluorine. Thus, the electronic energies of $AlHF_3^-$ and AlF_4^- are within 1 kcal/mol of what would be predicted be using the energy of $AlH_2F_2^-$ and adding the energy difference between AlH_3F^- and $AlH_2F_2^-$ either once ($AlHF_3^-$) or twice (AlF_4^-). In contrast, whereas the effects of the first two fluorines on energies of the alanes are nearly additive (to within 0.5 kcal/mol), the energy of AlF_3 is higher (less negative) than the additivity value by nearly 0.2 eV. Although Fig. 2 shows that the charge density is not exactly linearly related to the number of fluorines in the alanes, it does not account for the difference in energies, and particularly the energy of AlF_3. That difference accounts for most of the deviation from linearity in the CCSD(T) fluoride affinities shown in Fig. 2. The origin of the non-additive effect of fluorine in AlF_3 is not clear.

5. Conclusions

Fluorination of alanes increases the fluoride affinity, and hence the Lewis acidity, by increasing the extent of positive charge character on the aluminum atom. The increase in fluoride affinity is not linear because the energies of fluorinated alanes are not linear with increased number of fluorines. The measured fluoride affinities agree well with theoretically predicted values.

Acknowledgements

This work was supported by the National Science Foundation (CHE04-54874 and CHE08-08964). Thanks also to the donors of the Petroleum Research Fund, administered by the American Chemical Society, for partial support. Calculations were carried out using the resources of the Center for Computational Studies of Open-Shell and Electronically Excited Species (iopenshell.usc.edu), supported by the National Science Foundation through the CRIF:CRF program.

Appendix A. Supplementary data

Supplementary data associated with this article can be found, in the online version, at doi:10.1016/j.ijms.2010.09.003.

References

[1] P.G. Wenthold, Toward the systematic decomposition of benzene, Angew. Chem. Int. Ed. 44 (2005) 7170–7172.
[2] J.C. Haartz, D.H. McDaniel, Fluoride ion affinity of some Lewis acids, J. Am. Chem. Soc. 95 (1973) 8562–8565.
[3] J.W. Larson, T.B. McMahon, Strong hydrogen bonding in gas-phase anions. An ion cyclotron resonance determination of fluoride binding energetics to bronsted acids from gas-phase fluoride exchange equilibria measurements, J. Am. Chem. Soc. 105 (1983) 2944–2950.
[4] K.C. Lobring, C.E. Check, L.S. Sunderlin, The fluoride affinity of SO_2, Int. J. Mass Spectrom. 222 (2003) 221–227.
[5] P.G. Wenthold, R.R. Squires, Bond dissociation energies of F_2^- and HF_2^-. A gas phase experimental and G2 theoretical study, J. Phys. Chem. 99 (1995) 2002–2005.
[6] I.H. Krouse, H.A. Lardin, P.G. Wenthold, Gas-phase ion chemistry and ion thermochemistry of phenyltrifluorosilane, Int. J. Mass Spectrom. 227 (2003) 303–314.
[7] R. Zidan, B. Garcia-Diaz, C. Fewox, A. Stowe, J. Gray, A. Harter, Aluminum hydride: a reversible material for hydrogen storage, Chem. Commun. (2009) 3717–3719.
[8] P.J. Marinelli, J.A. Paulino, L.S. Sunderlin, P.G. Wenthold, J.C. Poutsma, A tandem selected ion flow tube-triple quadrupole instrument, Int. J. Mass Spectrom. Ion Processes 130 (1994) 89–105.
[9] N. Hallowitta, D. Carl, P.B. Armentrout, M.T. Rodgers, Dipole effects on cation-pi interactions: absolute bond dissociation energies of complexes of alkali metal cations to n-methylaniline and n,n-dimethyaniline, J. Phys. Chem. A 112 (2008) 7996–8008.
[10] K.M. Ervin, P.B. Armentrout, Translational energy dependence of $Ar^+ + XY \rightarrow ArX^+ + Y$ ($XY = H_2$, D_2, HD) from thermal to 30 eV cm, J. Chem. Phys. 83 (1985) 166.
[11] R.H. Schultz, K.C. Crellin, P.B. Armentrout, Sequential bond energies of iron carbonyl $Fe(CO)_x^+$ ($x = 1–5$): systematic effects on collision-induced dissociation measurements, J. Am. Chem. Soc. 113 (1991) 8590.
[12] L.S. Sunderlin, P.B. Armentrout, Thermochemistry of titanium(1+)-hydrocarbon bonds: translational energy dependence of the reactions of Ti+ with ethane propane, and trans-2-butene, Int. J. Mass Spectrom. Ion Processes 94 (1989) 149.

[13] M.J. Frisch, G.W. Trucks, H.B. Schlegel, G.E. Scuseria, M.A. Robb, J.R. Cheeseman, J.A. Montgomery Jr., T. Vreven, K.N. Kudin, J.C. Burant, J.M. Millam, S.S. Iyengar, J. Tomasi, V. Barone, B. Mennucci, M. Cossi, G. Scalmani, N. Rega, G.A. Petersson, H. Nakatsuji, M. Hada, M. Ehara, K. Toyota, R. Fukuda, J. Hasegawa, M. Ishida, T. Nakajima, Y. Honda, O. Kitao, H. Nakai, M. Klene, X. Li, J.E. Knox, H.P. Hratchian, J.B. Cross, V. Bakken, C. Adamo, J. Jaramillo, R. Gomperts, R.E. Stratmann, O. Yazyev, A.J. Austin, R. Cammi, C. Pomelli, J.W. Ochterski, P.Y. Ayala, K. Morokuma, G.A. Voth, P. Salvador, J.J. Dannenberg, V.G. Zakrzewski, S. Dapprich, A.D. Daniels, M.C. Strain, O. Farkas, D.K. Malick, A.D. Rabuck, K. Raghavachari, J.B. Foresman, J.V. Ortiz, Q. Cui, A.G. Baboul, S. Clifford, J. Cioslowski, B.B. Stefanov, G. Liu, A. Liashenko, P. Piskorz, I. Komaromi, R.L. Martin, D.J. Fox, T. Keith, M.A. Al-Laham, C.Y. Peng, A. Nanayakkara, M. Challacombe, P.M.W. Gill, B. Johnson, W. Chen, M.W. Wong, C. Gonzalez, J.A. Pople, Gaussian 03, Revision D.01, Gaussian, Inc., Wallingford, CT, 2004.
[14] M.T. Rodgers, K.M. Ervin, P.B. Armentrout, Statistical modeling of collision-induced dissociation thresholds, Chem. Phys. 106 (1997) 4499.
[15] K.M. Ervin, P.B. Armentrout, J. Chem. Phys. 83 (1985) 166.
[16] M.T. Rodgers, P.B. Armentrout, Statistical modeling of competitive threshold collision-induced dissociation, J. Chem. Phys. 109 (1998) 1787.
[17] H.J. Werner, P.J. Knowles, R. Lindh, F.R. Manby, M. Schutz, P. Celani, T. Korona, A. Mitrushenkov, G. Rauhut, T.B. Adler, R.D. Amos, A. Bernhardsson, A. Berning, D.L. Cooper, M.J.O. Deegan, A.J. Dobbyn, F. Eckert, E. Goll, C. Hampel, G. Hetzer, T. Hrenar, G. Knizia, C. Koppl, Y. Liu, A.W. Lloyd, R.A. Mata, A.J. May, S.J. McNicholas, W. Meyer, M.E. Mura, A. Nicklass, P. Palmieri, K. Pfluger, R. Pitzer, M. Reiher, U. Schumann, H. Stoll, A.J. Stone, R. Tarroni, T. Thorsteinsson, M. Wang, A. Wolf, MOLPRO, Version 2009.1, A Package of Ab Initio Programs, 2009.
[18] M. Nikitin, N. Igolkina, E. Skokan, I. Sorokin, L. Sidirov, Enthalpies of formation of the AlF4-ion, Russ. J. Phys. Chem. 60 (1986) 22–24.
[19] W. Kutzelnigg, J.D. Morgan, J. Phys. Chem. 96 (1992).
[20] A. Artau, K.E. Nizzi, B.T. Hill, L.S. Sunderlin, P.G. Wenthold, Bond dissociation energy in trifluoride ion, J. Am. Chem. Soc. 122 (2000) 10667–10670.
[21] A.E. Reed, P.V.R. Schleyer, Chemical bonding in hypervalent molecules. The dominance of ionic bonding and negative hyperconjugation over d-orbital participation, J. Am. Chem. Soc. 112 (1990) 1434–1445.
[22] A.E. Reed, R.B. Weinstock, F. Weinhold, Natural population analysis, J. Chem. Phys. 83 (1985) 735–746.
[23] J.P. Foster, F. Weinhold, Natural hybrid orbitals, J. Am. Chem. Soc. 102 (1980) 7211–7218.